ChemComm

Accepted Manuscript

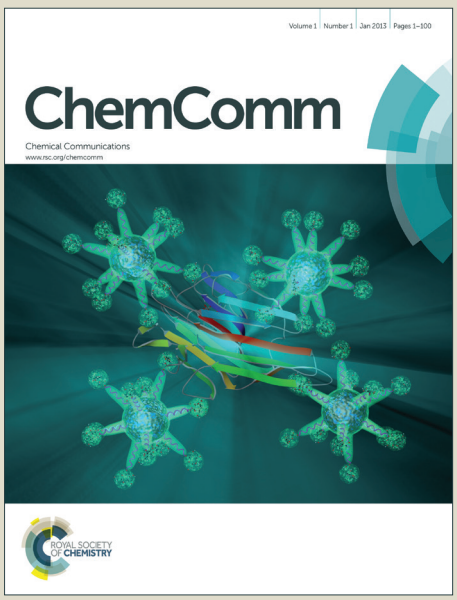

ROYAL SOCIETY OF CHEMISTRY

www.rsc.org/chemcomm

Atomic layer deposition on 2D transition metal chalcogenides: Layer dependent reactivity and seeding with organic ad-layers

Christian Wirtz,[a,b] Toby Hallam,[b] Conor Cullen,[a,b] Nina C. Berner,[a,b] Maria O'Brien,[a,b] Mario Marcia,[c] Andreas Hirsch,[c] and Georg S Duesberg*[a,b]

Received Xth XXXXXXXXXX 20XX, Accepted Xth XXXXXXXXX 20XX
First published on the web Xth XXXXXXXXXX 200X
DOI: 10.1039/b000000x

This commmunication presents a study of atomic layer deposition of Al_2O_3 on transition metal dichalcogenide (TMD) two-dimensional films which is crucial for use of these promising materials for electronic applications. Deposition of Al_2O_3 on pristine chemical vapour deposited MoS_2 and WS_2 crystals is demonstrated. This deposition is dependent on the number of TMD layers as there is no deposition on pristine monolayers. In addition, we show that it is possible to reliably seed the deposition, even on the monolayer, using non-covalent functionalisation with perylene derivatives as anchor unit.

The integration of transition metal dichalcogenides (TMDs) into existing semiconductor technology is of major interest.[1,2] The synthesis of these materials has been vastly improved over the last few years and many possible devices have been proposed and realised.[3–6] But to finally achieve their large-scale integration and production, it is necessary to make TMDs fully CMOS processable. One prerequisite for this is the deposition of subsequent layers on top of the TMD for gating and passivation as the performance and stability of TMD based devices hugely depends on their dielectric environment. This task is non-trivial as any impact on the surface of the TMD will result in the destruction of its electronic properties. It has been shown that encapsulation of the 2D material by mechanical deposition of hexagonal boron nitride results in the best preservation of its electronic properties but this approach is not scalable.[7]

Other frequently used deposition methods for oxides such as sputtering or plasma-enhanced chemical vapour deposition (PECVD) are not suitable as their application will cause damage to the monolayer.

Atomic layer deposition (ALD) is a mild and highly precise technique for thin film deposition, mainly used for depositing gate oxides in integrated circuits.[8] The most common ALD process is the deposition of Al_2O_3 from alternating exposures of trimethylaluminium (TMA, $Al(CH_3)_3$) and water according to the reaction[9]:

$$2\,Al(CH_3)_3 + 3\,H_2O \longrightarrow Al_2O_3 + 6\,CH_4 \;\; \Delta H = -376 kcal$$

This reaction is thermodynamically highly favourable and works over a large range of temperatures with temperatures between 33 °C and 500 ° demonstrated, making it very reliable and common in the silicon and III-V semiconductor industries.[10,11] However, in the initial step the TMA needs a surface hydroxyl group with which it reacts and the lack of such groups on the TMD's basal plane makes starting the deposition non-trivial; a challenge also encountered with graphene.[12–15] Using ozone instead of water may prove harmful to the oxidation-sensitive TMD layers, though there have been some recent successes.[16] An initial, purely adsorption-based deposition can be achieved but tends to be dependent on temperature and other factors like underlying electronic structure and is therefore often not entirely reproducible; it has been shown several times that studies may not reproduce results under apparently similar conditions.[12,17,18]

In this study we used single crystalline layers of MoS_2 and WS_2 grown via chemical vapour deposition (CVD) as previously demonstrated.[19] The ALD on those layers was performed at the relatively low temperature of 80 °C with 27 cycles of TMA and H_2O using 0.5 second pulses with 20 seconds purge time (60 sccm N_2) and should yield ∼3 nm of Al_2O_3. Those samples were analysed with atomic force microscopy (AFM) to determine step heights and scanning Raman spectroscopy. Al_2O_3 as deposited by ALD does not exhibit a Raman signal but both MoS_2 and WS_2 have characteristic peaks in the region from 370 cm^{-1} to 420 cm^{-1}.

The MoS_2 and WS_2 layers have the characteristic triangular shape and consisted of mostly monolayer except for the flake centre which occasionally exhibited an onset of multilayer growth. This can be seen in the different contrast regions shown in figure 1a. An AFM scan (figure 1b), along with the line scans in figure 1c and d, shows the ideal step height of

[a] *School of Chemistry, Trinity College Dublin, Dublin, Ireland; Tel: +353 1 896 3035; E-mail: duesberg@tcd.ie*
[b] *CRANN & AMBER institues, Trinity College, Dublin, Ireland*
[c] *Department of Chemistry and Pharmacy, Organische Chemie II, Friedrich-Alexander Universität Erlangen-Nürnberg, Henkestrasse 42, 91054 Erlangen, Germany*

0.7 nm per TMD layer. This proved to be very useful as it allowed for side-by-side comparison of Al_2O_3 ALD on mono- and bilayer samples.

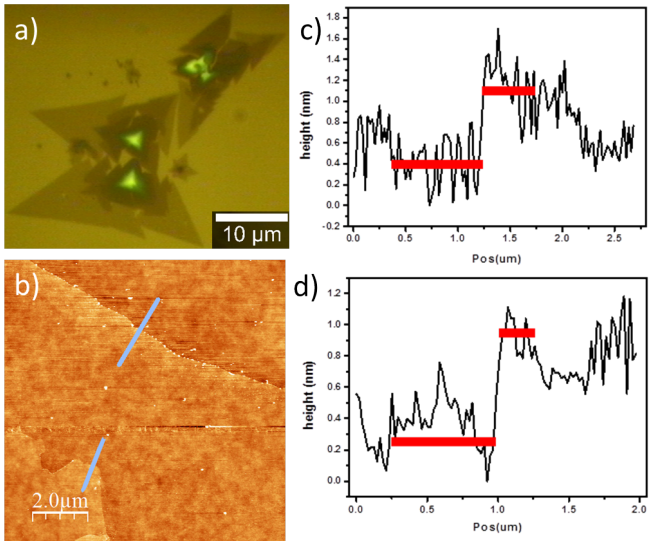

Fig. 1 Representation of the MoS_2 flakes used in the experiment: a) Optical image of flakes consisting of crystalline monolayers and some multilayers in the flake centres. b) AFM image of a MoS_2 flake; c) and d) show the line profiles along the marked lines in b) with a step height of 0.7 nm.

In figure 2a we present an AFM image of a triangular WS_2 flake on SiO_2 after 3 nm Al_2O_3 deposition. It is apparent that the triangular flake (dark region) is lower than the surrounding substrate. This becomes better visible in the line profile across the flake as shown in figure 2b. The step height between the flake and substrate is ∼2.3 nm after deposition, perfectly corresponding to the difference of 3nm Al_2O_3 deposition minus the flake height of 0.7 nm. Thus there is no deposition of Al_2O_3 on the monolayer. The double-layered centre of the flake increased in height to ∼3.7 nm with respect to the monolayer, perfectly corresponding to 0.7 nm flake height plus 3 nm Al_2O_3. At the edge of the monolayer Al_2O_3 was deposited which we attribute to dangling bonds and defects that are more reactive. This high selectivity in the deposition process was found in both both WS_2 and MoS_2 single crystals grown via CVD. This is to our knowledge the first observation of selective chemical behaviour between mono- and double-layered or multilayered TMDs. We attribute this selectivity to two factors: Firstly, our films must be extremely clean with no defects in the basal plane as otherwise the ALD would occur at those centres like at the flake edge. As the films came straight out of the oven and there was no transfer, no polymer residue could seed any ALD, something that may be responsible for the inconsistent results in the field so far. Secondly, TMDs undergo a significant change in electronic structure when going from multi-layered structures to single layers.[20,21] There is a change from indirect bandgap of 1.2 eV and 1.3 eV to a direct bandgap of 1.9 eV and 2 eV for MoS_2 and WS_2, respectively.[22,23] Hence the initially adsorption-based ALD may be so heavily influenced by this difference in underlying electronic structure that it is significantly different for monolayers in comparison to bulk. However, theoretical modelling is required to further investigate the underlying mechanism. This selectivity can be a significant advantage: Covering all layers but the monolayer with a dielectric leaves only the material with the direct bandgap exposed. This provides a novel pathway to select monolayer regions and can be used for vertical device fabrication and selective chemistry.

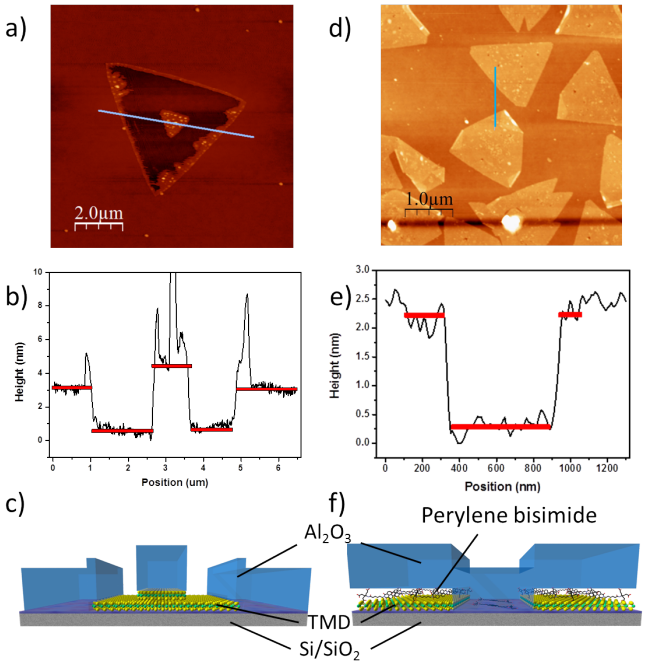

Fig. 2 a) AFM analysis of TMDs after ALD. a) Topography of a WS_2 triangle after 27 cycles of TMA and H_2O. The monolayer part of the triangle lies lower than the surrounding SiO_2. b) Line profile along the marked line in a). The step height between monolayer WS_2 and SiO_2 is 2.3 nm and between monolayer WS_2 and bilayer WS_2 is 3.7 nm. Only the monolayer edges were covered with the expected 3 nm Al_2O_3. c) Schematic representation of the surface structure in a) as indicated by the AFM scan. d) Topography of MoS_2 triangles after 27 cycles of ALD after seeding with a perylene bisimide derivative. The flakes are higher than the surrounding substrate. b) Line profile along the line marked in d). The step height is 1.9 nm. f) Schematic representation of the structure of d) as indicated by the scan.

However, deposition of uniform dielectrics on monolayer TMDs is desired for passivation and electronic device fabrication. We therefore explore non-covalent functionalisation

of TMD basal planes with molecules that contain $-OH$ and $-COOH$ units which can react with TMA and thereby seed the reaction.[8,26]

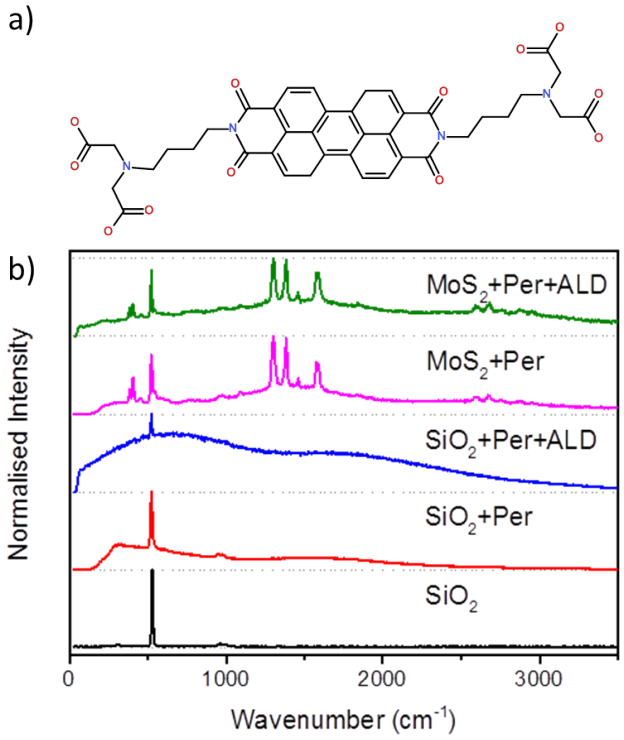

Fig. 3 a) Chemical structure of the perylene bisimide used for non-covalent functionalisation and ALD seeding. b) Normalised Raman spectra of the samples at various stages: The SiO_2 spectrum only shows the standard strong peak at 521 cm^{-1}. Upon functionalisation with perylene bisimide a strong fluorescent background is observed. This remains after ALD. On the TMD the perylene shows several intense peaks in the region of 1300 cm^{-1} to 1600 cm^{-1} and around 2700 cm^{-1} while the MoS_2 has its peaks at $\sim$400 cm^{-1}. All these peaks remain after ALD.

We use a perylene-based anchor unit on our TMDs.[27] This perlyene, shown in figure 3a, has a large aromatic core that can non-covalently attach to the TMD and end-groups with hydroxy and carboxyl functionalities. It is similar to molecules that have been employed to seed these depositions on graphene by Alaboson *et al* with the difference that our molecule has longer end-group chains with carboxylic acid groups.[28] This kind of end-group has been shown to seed Al_2O_3 ALD from TMA and H_2O.[29] The perylene adsorbs very strongly on TMDs and is deposited from an aqueous pH7 buffer solution by simple dip-coating. Washing the sample with water after deposition leaves only a thin layer of perylenes on MoS_2 and WS_2. As can be seen in the AFM scan in figure 2d, ALD on a perylene-covered sample leads to a perfectly homogeneous deposition of Al_2O_3 on all layers of MoS_2. The topological cross-section in figure 2e reveals that the step height between MoS_2 flake and SiO_2 substrate is not 0.7 nm any more but around 1.9 nm. The additional height difference of 1.2 nm implies that the perylene adsorbs better on the TMDs than on SiO_2 and that it may be in an upright conformation rather than laying flat.

To investigate the effect of ALD on the TMD we utilised scanning Raman spectroscopy. The Raman spectra of both MoS_2 and WS_2 are very similar, with two peaks closely spaced in the region around 400 cm^{-1}, shown for MoS_2 in figure 4d. Change in molecular or electronic structure due to Al_2O_3 deposition should result in an alteration of those signals.[24] The out-of-plane Raman active vibration of MoS_2 at 405-410 cm^{-1} has previously been shown to shift with layer number and doping[25]. A shift with layer number is expectedly observed as shown in figure 4a but no further shift upon Al_2O_3 deposition occurs as shown in figure 4b. Hence the electronic structure of the multilayer (coated) and monolayer (uncoated) TMD appears unperturbed upon Al_2O_3 deposition.

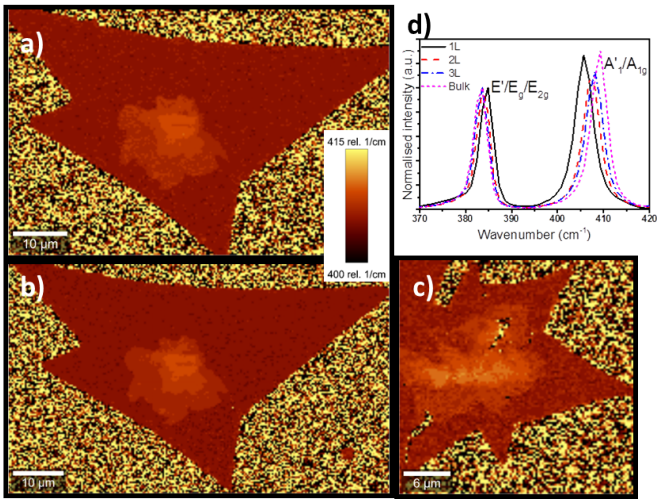

Fig. 4 Mapped out Raman spectrographs of MoS_2 flakes. Shown is the MoS_2 A1g peak position whose shift indicates different layer numbers and doping levels. a) Pristine MoS_2, the central area of the flake shows multilayer signal; b) the same MoS_2 flake after exposure to 27 cycles of TMA and H_2O, yielding 3 nm thick Al_2O_3; there is no appreciable change, indicating the exposure had no impact on electronic structure. c) A different MoS_2 flake after perylene deposition and exposure to ALD shows a slight blueshift, possibly indicating some p-doping. d) Average spectra of the different regions of the flake in a).

Raman mapping of the TMD's "A" peak (figure 4c) shows that the MoS_2 and WS_2 are not damaged by the deposition and retain their characteristics although there is a minor blueshift of $\sim$1 cm^{-1}, potentially indicating p-doping.[24,30] As this is at

our spectrometer's resolution limit it will require further investigation.

Investigation of the perylene bisimide's Raman spectrum, shown in figure 3b, shows several features. On just SiO_2 it has a very strong fluorescent background and does not show any features. After ALD this fluorescence remains, indicating the continued presence of the perylene. On TMDs it shows several peaks in the regions around 1500 cm^{-1} and 2700 cm^{-1} which remain after ALD, confirming its presence at all stages. This makes the interpretation of the 1.9 nm step height from figure 2e difficult and indicates different molecular orientations on SiO_2 and MoS_2.

In summary, we demonstrated that there exists selective chemistry of monolayer TMD surfaces over their multilayer counterparts. We have shown that this can lead to the selective deposition of Al_2O_3 which is essentially a method to selectively mask all areas but monolayer of MoS_2 and WS_2. This will hopefully lead to a whole variety of layer number selective chemistry in future. Furthermore we demonstrated that an easily accessible, non-covalent functionalisation with perylene derivatives allows for reliable ALD of Al_2O_3 on monolayer TMDs without damage to their electronic integrity as observed by Raman spectroscopy. These findings are an important step forward toward integration of TMDs in real devices.

Acknowledgements The authors thank Science Foundation Ireland for funding under the grant SFI-Pica:Pi_10/IN.1/I3030.

References

1 D. Jariwala, V. K. Sangwan, L. J. Lauhon, T. J. Marks and M. C. Hersam, *ACS Nano*, 2014, **8**, 1102–1120.

2 A. C. Ferrari, F. Bonaccorso, V. Fal'ko, K. S. Novoselov, S. Roche, P. Boggild, S. Borini, F. H. L. Koppens, V. Palermo, N. Pugno, J. A. Garrido, R. Sordan, A. Bianco, L. Ballerini, M. Prato, E. Lidorikis, J. Kivioja, C. Marinelli, T. Ryhanen, A. Morpurgo, J. N. Coleman, V. Nicolosi, L. Colombo, A. Fert, M. Garcia-Hernandez, A. Bachtold, G. F. Schneider, F. Guinea, C. Dekker, M. Barbone, Z. Sun, C. Galiotis, A. N. Grigorenko, G. Konstantatos, A. Kis, M. Katsnelson, L. Vandersypen, A. Loiseau, V. Morandi, D. Neumaier, E. Treossi, V. Pellegrini, M. Polini, A. Tredicucci, G. M. Williams, B. Hee Hong, J.-H. Ahn, J. Min Kim, H. Zirath, B. J. van Wees, H. van der Zant, L. Occhipinti, A. Di Matteo, I. A. Kinloch, T. Seyller, E. Quesnel, X. Feng, K. Teo, N. Rupesinghe, P. Hakonen, S. R. T. Neil, Q. Tannock, T. Lofwander and J. Kinaret, *Nanoscale*, 2015, **7**, 4598–4810.

3 H. R. Gutiérrez, N. Perea-López, A. L. Elías, A. Berkdemir, B. Wang, R. Lv, F. López-Urías, V. H. Crespi, H. Terrones and M. Terrones, *Nano Letters*, 2013, **13**, 3447–3454.

4 Y. Gong, J. Lin, X. Wang, G. Shi, S. Lei, Z. Lin, X. Zou, G. Ye, R. Vajtai, B. I. Yakobson, H. Terrones, M. Terrones, B. Tay, J. Lou, S. T. Pantelides, Z. Liu, W. Zhou and P. M. Ajayan, *Nat Mater*, 2014, **13**, 1135–1142.

5 X. Duan, C. Wang, J. C. Shaw, R. Cheng, Y. Chen, H. Li, X. Wu, Y. Tang, Q. Zhang, A. Pan, J. Jiang, R. Yu, Y. Huang and X. Duan, *Nat Nano*, 2014, **9**, 1024–1030.

6 A. M. van der Zande, P. Y. Huang, D. A. Chenet, T. C. Berkelbach, Y. You, G.-H. Lee, T. F. Heinz, D. R. Reichman, D. A. Muller and J. C. Hone, *Nat Mater*, 2013, **12**, 554–561.

7 T. Roy, M. Tosun, J. S. Kang, A. B. Sachid, S. B. Desai, M. Hettick, C. C. Hu and A. Javey, *ACS Nano*, 2014, **8**, 6259–6264.

8 S. M. George, *Chemical Reviews*, 2010, **110**, 111–131.

9 R. L. Puurunen, *Journal of Applied Physics*, 2005, **97**, 121301.

10 M. D. Groner, F. H. Fabreguette, J. W. Elam and S. M. George, *Chemistry of Materials*, 2004, **16**, 639–645.

11 R. Matero, A. Rahtu, M. Ritala, M. Leskelä and T. Sajavaara, *Thin Solid Films*, 2000, **368**, 1–7.

12 H. Liu, K. Xu, X. J. Zhang and P. D. Ye, *Applied Physics Letters*, 2012, **100**, 152115.

13 B. Dlubak, P. R. Kidambi, R. S. Weatherup, S. Hofmann and J. Robertson, *Applied Physics Letters*, 2012, **100**, 173113.

14 J. Kim and S. Jandhyala, *Thin Solid Films*, 2013, **546**, 85–93.

15 S. McDonnell, B. Brennan, A. Azcatl, N. Lu, H. Dong, C. Buie, J. Kim, C. L. Hinkle, M. J. Kim and R. M. Wallace, *Acs Nano*, 2013, **7**, 10354–10361.

16 L. X. Cheng, X. Y. Qin, A. T. Lucero, A. Azcatl, J. Huang, R. M. Wallace, K. Cho and J. Kim, *Acs Applied Materials & Interfaces*, 2014, **6**, 11834–11838.

17 S. Brunauer, P. H. Emmett and E. Teller, *Journal of the American Chemical Society*, 1938, **60**, 309–319.

18 J. Yang, S. Kim, W. Choi, S. H. Park, Y. Jung, M. H. Cho and H. Kim, *Acs Applied Materials & Interfaces*, 2013, **5**, 4739–4744.

19 M. O'Brien, N. McEvoy, T. Hallam, H.-Y. Kim, N. C. Berner, D. Hanlon, K. Lee, J. N. Coleman and G. S. Duesberg, *Sci. Rep.*, 2014, **4**, 7374.

20 K. F. Mak, C. Lee, J. Hone, J. Shan and T. F. Heinz, *Physical Review Letters*, 2010, **105**, 136805.

21 W. Zhao, Z. Ghorannevis, L. Chu, M. Toh, C. Kloc, P.-H. Tan and G. Eda, *ACS Nano*, 2013, **7**, 791–797.

22 A. M. Goldberg, A. R. Beal, F. A. Lvy and E. A. Davis, *Philosophical Magazine*, 1975, **32**, 367–378.

23 A. L. Elías, N. Perea-López, A. Castro-Beltrán, A. Berkdemir, R. Lv, S. Feng, A. D. Long, T. Hayashi, Y. A. Kim, M. Endo, H. R. Gutiérrez, N. R. Pradhan, L. Balicas, T. E. Mallouk, F. López-Urías, H. Terrones and M. Terrones, *ACS Nano*, 2013, **7**, 5235–5242.

24 B. Chakraborty, A. Bera, D. V. S. Muthu, S. Bhowmick, U. V. Waghmare and A. K. Sood, *Physical Review B*, 2012, **85**, 161403.

25 H. Li, Q. Zhang, C. C. R. Yap, B. K. Tay, T. H. T. Edwin, A. Olivier and D. Baillargeat, *Advanced Functional Materials*, 2012, **22**, 1385–1390.

26 X. R. Wang, S. M. Tabakman and H. J. Dai, *Journal of the American Chemical Society*, 2008, **130**, 8152–+.

27 M. Marcia, P. Singh, F. Hauke, M. Maggini and A. Hirsch, *Org. Biomol. Chem.*, 2014, **12**, 7045–7058.

28 J. M. P. Alaboson, Q. H. Wang, J. D. Emery, A. L. Lipson, M. J. Bedzyk, J. W. Elam, M. J. Pellin and M. C. Hersam, *ACS Nano*, 2011, **5**, 5223–5232.

29 M. Li, M. Dai and Y. J. Chabal, *Langmuir*, 2009, **25**, 1911–1914.

30 Y. Shi, J.-K. Huang, L. Jin, Y.-T. Hsu, S. F. Yu, L.-J. Li and H. Y. Yang, *Sci. Rep.*, 2013, **3**, 1839.